International Immunopharmacology 75 (2019) 105816

Contents lists available at ScienceDirect

International Immunopharmacology

journal homepage: www.elsevier.com/locate/intimp

Docosahexaenoic acid inhibits hepatic stellate cell activation to attenuate liver fibrosis in a PPARγ-dependent manner

Jianlin He[a,b], Bihong Hong[a], Mianli Bian[b], Huanhuan Jin[b,c], Junde Chen[a], Jiangjuan Shao[b], Feng Zhang[b,*], Shizhong Zheng[b,*]

[a] Third Institute of Oceanography, Ministry of Natural Resources, Xiamen 361005, PR China
[b] Department of Pharmacology, School of Pharmacy, Nanjing University of Chinese Medicine, Nanjing 210029, PR China
[c] Department of Pharmacology, School of Pharmacy, Wannan Medical College, Wuhu 241000, PR China

ARTICLE INFO

Keywords:
Docosahexaenoic acid
Liver fibrosis
Peroxisome proliferator-activated receptor γ
Molecular docking
Hepatic stellate cells
Ligand activation

ABSTRACT

Docosahexaenoic acid (DHA) has been found to have a hepatoprotective effect. In this study, we investigated the role of peroxisome proliferator-activated receptor γ (PPARγ) in DHA regulation of liver fibrosis. DHA was found to inhibit hepatic stellate cell (HSC)-LX2 cell viability and downregulate marker proteins of HSC activation. Furthermore, DHA induced cell cycle arrest at G1 phase in HSCs. Antagonism of PPARγ by GW9662 abrogated the effects of DHA on HSCs. Computer-aided molecular docking predicted that DHA bound to PPARγ via hydrogen bonding with residues Ser289, His323, Tyr473, and His499. We overexpressed Ser289 mutant PPARγ in HSC-LX2 cells and investigated fibrotic marker modulation, and found that DHA effects on HSCs were diminished. Thus, bonding with the Ser289 residue might be indispensable for DHA to activate PPARγ to exert its inhibiting effect on activated HSCs. Last, data from a CCl_4-treated mouse model confirmed that PPARγ activation was required for DHA to attenuate liver fibrosis.

1. Introduction

Liver fibrosis is the common pathological stage of chronic liver diseases. Advanced fibrosis might develop into life-threatening cirrhosis and hepatocellular carcinoma [1]. During the development of liver fibrosis, hepatic stellate cells (HSCs) are activated and convert into fibroblasts to produce collagen and thus propagate fibrosis. However, compelling evidence indicates that liver fibrosis is reversible [2]. It is believed that HSC reversion is a promising strategy to treat liver fibrosis. HSC activation and conversion are modulated by multiple factors and pathways [3]. Notably, PPARγ is highly expressed in quiescent HSCs of a normal liver. Upon HSC activation, PPARγ expression and activity are dramatically reduced [4]. In contrast, restoration of PPARγ reverses HSC activation to a "quiescent" phenotype [5]. Thus, PPARγ is a key molecule modulating HSC activation.

ω-3 polyunsaturated fatty acids (PUFAs) have multiple beneficial effects such as the reduction of cardiovascular diseases [6] and neuroprotection [7]. Previously, we found that DHA free acid attenuates CCl_4-induced liver fibrosis in rats [8]. However, little is known about the effect of DHA on HSCs that are the primary target of antifibrotic therapies [9].

As a long chain ω-3 PUFA, DHA is a natural ligand of PPARγ [10]. The role of PPARγ in DHA effects on liver fibrosis is not fully understood. Based on our previous study, we hypothesized that DHA might inhibit HSC activation by activating PPARγ to attenuate liver fibrosis. In this study, we investigated the molecular mechanism and potential target of DHA intervention in HSC activation during liver fibrosis by experimental and molecular simulation approaches.

2. Materials and methods

2.1. Chemicals and antibodies

Docosahexaenoic acid ($C_{22}H_{32}O_2$, purity: > 99%) was obtained from Nu-chek Prep (Elysian, MN, USA). GW9662 ($C_{13}H_9ClN_2O_3$; purity: > 99.88%) was obtained from Selleck Chemicals (Houston, TX, USA). Primary antibodies against α-Smooth muscle actin (α-SMA), fibronectin, PPARγ, transforming growth factor β type I receptor (Tβ-RI), transforming growth factor β type II receptor (Tβ-RII), platelet-derived growth factor β receptor (PDGF-βR) were purchased from Abcam (Cambridge, MA, USA). Antibodies against p27 and p21 were purchased from Proteintech (Rosemont, IL, USA). An antibody against β-actin was purchased from Bioworld (St. Louis Park, MN, USA).

* Corresponding authors at: 138 Xianlin Avenue, Nanjing 210023, Jiangsu, PR China.
E-mail addresses: nucmzf@163.com (F. Zhang), nytws@163.com (S. Zheng).

https://doi.org/10.1016/j.intimp.2019.105816
Received 28 May 2019; Received in revised form 16 July 2019; Accepted 9 August 2019
Available online 19 August 2019

2.2. Cell culture and DHA treatment of HSC-LX2 cells

The human HSC-LX2 cell line was obtained from the Cell Bank of the Chinese Academy of Sciences (Shanghai, China). Cells were cultured in Dulbecco's modified Eagle's medium (DMEM) with 10% fetal bovine serum (FBS) and grown in a 5% CO_2 humidified atmosphere at 37 °C. The cells were subjected to no more than 20 passages. A stock solution of DHA in ethanol was stored at −20 °C and diluted in complete growth medium before experiments (final concentration of ethanol: 0.05% v/v). Cells were treated with ethanol as a control or DHA at various concentrations for 24 h in complete growth medium.

2.3. MTT assay

LX-2 cells at 1×10^5 cells mL^{-1} were seeded in 96-well plates and cultured in DMEM supplemented with 10% FBS. At 60% confluence, the cells were treated with DHA at the indicated concentrations for 24, 48, and 72 h. After treatments, the assay was performed according to the protocol provided by the manufacturer (Promega, Madison, WI).

2.4. Flow cytometric analysis of the cell cycle

HSCs at about 1×10^5 cells mL^{-1} were seeded in 6-well plates and treated with DHA at the indicated concentrations for 24 h. According to the manufacturer's instructions, the cell cycle was analyzed using a cellular DNA flow cytometric kit (Nanjing KeyGen Biotech, Nanjing, China). Percentages of HSCs in each cell cycle phase (G0/G1, S, and G2/M) were determined by flow cytometry (FACSCalibur, Becton, Dickinson and Company, Franklin Lakes, NJ, USA). The data were analyzed with FlowJo 10 software (Ashland, OR, USA). The experiments were performed in triplicate and representative histogram graphs are shown.

2.5. Animal procedures and treatments

Five-week-old male ICR mice (Qinglongshan Animal Breeding Center, Nanjing, China) weighting 18–22 g were divided into five groups randomly (n = 8). All animals were housed in a temperature- and humidity-controlled environment with a 12 h light/dark cycle and fed a standard mouse diet. Group 1 was the normal control, in which mice were intraperitoneally (i.p.) injected with olive oil (6 mL/kg). Group 2 was the DHA control, in which mice were i.p. injected with olive oil (6 mL/kg) and intragastrically (i.g.) treated with DHA (20 mg/kg). Group 3 was the model group, in which the mice were i.p. injected with CCl_4 [20% (v/v) in olive oil, 6 mL/kg]. Group 4 was the DHA treatment group, in which mice received 20% CCl_4 (i.p.) at 6 mL/kg and DHA (i.g.) at 20 mg/kg. Group 5 was the DHA + GW9662 group, in which mice were treated with 20% CCl_4 (6 mL/kg i.p.), GW9662 (3 mg/kg, i.g.), and DHA (20 mg/kg, i.g.). Groups 3–5 were i.p. injected with CCl_4 three times a week for 4 weeks to induce liver fibrosis. Groups 2, 4, and 5 were treated with DHA once daily. Group 5 was treated with GW9662 at 1 h before DHA treatment once daily. DHA or GW9662 were dissolved in 0.5% carboxymethylcellulose sodium (CMC-Na) as a stock solution and suspended in sterile saline to adjust the concentration to 20 or 3 mg/kg body weight, respectively, every day before treatment. After 4 weeks of administration, mice were anaesthetized by inhalation of ether, and blood was collected via the retro orbital sinus. Then, the mice were sacrificed by decapitation and then their livers were isolated by surgery in a separate room from the other animals. Efforts were made to minimize animal suffering as much as possible. A small portion of the liver was removed for histopathology. All protocols were approved by the Institutional and Local Committee on the Care and Use of Animals of Nanjing University of Chinese Medicine. All mice received humane care according to the National Institutes of Health (USA) guidelines.

2.6. Liver histopathology

Liver tissues were fixed in 10% neutral buffered formalin and embedded in paraffin. Hematoxylin-eosin (HE) staining was performed for pathological examination by standard methods. Masson staining and Sirius Red staining were used for collagen assessment according to standard methods. Images were obtained in a blinded manner in random fields by a pathologist, and representative views of liver sections are shown.

2.7. Enzyme-linked immunosorbent assays (ELISAs)

TGF-β and PDGFbb levels in the culture medium were determined by ELISA kits purchased from Shanghai Biotechnology (Shanghai, China). Levels of serum aspartate aminotransferase (AST) and alanine aminotransferase (ALT) were determined by ELISA kits from Nanjing Jiancheng Bioengineering Institute (Nanjing, China), according to the protocols provided by the manufacturer. Serum levels of hyaluronic acid (HA), laminin (LN), procollagen type III (PCIII), and type IV collagen (ColIV) were determined using kits purchased from Shanghai Yuanye Bio-Technology (Shanghai, China). Hydroxyproline (HYP), interleukin (IL)-6, IL-8, tumor necrosis factor (TNF)-α, TGF-β, and PDGFbb levels in the liver were determined by kits from Shanghai Yuanye Bio-Technology.

2.8. Immunohistochemistry

Liver tissue sections were incubated with primary antibodies against CD45 and F4/80 for immunohistochemical evaluation by standard methods. Images were blindly obtained in random fields under a microscope (ZEISS Axio vert. A1, Germany). Representative views are shown.

2.9. Immunofluorescence analyses

Thin sections of liver tissues were blocked with 1% bovine serum albumin and incubated with primary antibodies overnight at 4 °C. After washing with PBS, sections on slides were incubated with fluorescent dye-conjugated secondary antibodies at room temperature for 2 h. Sections incubated with secondary antibodies alone were used as negative controls. For cell staining, HSC-LX2 cells were seeded in 6-well plates and treated with vehicle or various reagents at the indicated concentrations for 24 h. Cells were incubated with primary and secondary antibodies in succession, similar to the protocol described above. Finally, DAPI was used to stain the nuclei of cells. Images were obtained in random fields under a microscope (ZEISS Axio vert. A1). Representative views are shown.

2.10. Molecular simulation

Molecular docking was performed using GLIDE software (Schrödinger, LLC, New York, NY, USA). The X-ray crystal structures of PPARγ complexed with rosiglitazone or DHA were retrieved from the PDB database with PDB code 5JI0 or 2VV0, respectively. The Protein Preparation Wizard in GLIDE software was used to prepare the structure of PPARγ, which included assigning bond orders and water orientations, removing water molecules, adding hydrogens, and creating zero-order bonds to metals and disulfide bonds. The protein was then minimized using the OPLS3 force field with a default constraint of 0.30 Å root-mean-square deviation. A receptor grid was created before GLIDE docking. The three-dimensional structure of DHA was generated using the LigPrep module from Schrödinger with the default settings. For GLIDE docking, the Standard Precision mode was used. The top 10 ranking conformations for DHA were chosen in the output tab to set the output numbers. Images of the docking conformations were subsequently prepared using Pymol.

2.11. Site-directed mutagenesis and cell transfection

PCR-based site-directed mutagenesis was carried out to mutate the Ser289 residue to alanine in the human PPARγ gene (NCBI accession: NM_005037). The PCR product was subcloned between the *Xho*I and *Kpn*I sites of the mammalian expression vector GV230 (element sequence: CMV-MCS-EGFP-SV40-Neomycin) provided by Shanghai Genechem Co., Ltd. (Shanghai, China). PPARγ-mutant plasmids were generated using the QuickChange™ Site-Directed Mutagenesis Kit (Stratagene, La Jolla, CA, USA), according to the manufacturer's instructions with the following oligonucleotides: 5′-TACCGGACTCAG ATCTCGAGCGCCACCATGACCATGGTTGACACAGAGA-3′ (forward) and 5′-GATCCCGGGCCC GCGGTACCGTGTACAAGTCCTTGTAGATCTC CTG-3′ (reverse). Mutations were confirmed in positive colonies by DNA sequencing. Transfection was performed using Lipofectamine 2000 Transfection Reagent (Thermo Fisher Scientific, Waltham, MA, USA) in medium without serum or antibiotics for 24 h.

2.12. Western blot analyses

Whole cell protein extracts were prepared from HSCs with RIPA buffer. Protein bands were visualized using a chemiluminescence reagent (Millipore, Burlington, MA, USA). Equivalent loading was confirmed using the antibody against β-actin. The levels of target proteins were densitometrically determined by Quantity One 4.4.1 (Bio-Rad Laboratories, Hercules, CA, USA). Each analysis was performed in three independent experiments. Representative blots are shown.

2.13. Statistical analyses

Results were obtained from at least triplicate experiments. Data are presented as means ± SEM and were analyzed using SPSS 16.0 software. The significance of differences was determined by one-way ANOVA with Dunnett's post-hoc test. Values of $P < 0.05$ were considered to be statistically significant. Histograms were created using GraphPad Prism 5 software (San Diego, CA, USA).

3. Results

3.1. DHA suppresses LX-2 cell viability and inhibits their activation

Proliferation is a critical event of HSC activation [11]. We initially examined the effects of DHA on the viability of LX-2 cells, a well-validated immortalized human HSC line [12]. The MTT assays showed that DHA dose- and time-dependently reduced the viability of LX-2 cells (Fig. 1A). Furthermore, we examined the protein abundance of key markers of HSC activation, α-SMA [13] and fibronectin [14]. The results showed that DHA dose-dependently diminished their expression (Fig. 1B). Tβ-RI, Tβ-RII, and PDGF-βR are receptors that transmit profibrogenic signals [15,16]. Our western blot results showed that, except for Tβ-RII, DHA dose-dependently downregulated α-SMA, fibronectin, Tβ-RI, and PDGF-βR expression (Fig. 1B & C). Consistently, immunofluorescence showed that expression of α-SMA, fibronectin, Tβ-RI, and PDGF-βR was reduced by DHA treatment (Fig. 1D). Collectively, DHA suppressed LX-2 cell viability and inhibited their activation.

3.2. GW9662 abrogates the effects of DHA on LX-2 cell activation

Because DHA is a PPARγ ligand, we used the selective PPARγ inhibitor GW9662 to assess the involvement of PPARγ in the current experimental context. We found that addition of GW9662 (1 μM) abolished the inhibitive effects of DHA on the expression of α-SMA, fibronectin, Tβ-RI, and PDGF-βR (Fig. 2A). PDGFbb and TGF-β are considered to be the most potent cytokines that stimulate the proliferation and fibrogenesis of HSCs [17,18]. Therefore, we also detected their abundance in the culture medium. Interestingly, DHA did not significantly modulate PDGFbb or TGF-β levels in the culture medium, but their levels were highly elevated by GW9662 (Fig. 2B). We also observed that DHA enhanced PPARγ translocation, which was abrogated by GW9662 (Fig. 2C). Taken together, these findings indicated a PPARγ activation-dependent mechanism underlying DHA suppression of HSC activation.

3.3. DHA induces LX-2 cell cycle arrest at G1 phase in a PPARγ-dependent manner

The inhibition of cell viability could have been caused by cell cycle arrest. Therefore, we investigated the effect of DHA on the cell cycle of LX-2 cells by flow cytometry. We found that DHA dose-dependently induced accumulation of cells in G1 phase (Fig. 3A), but this effect was abolished by GW9662 (Fig. 3C). Moreover, cyclin-dependent kinase inhibitors p27 and p21 were upregulated by DHA (Fig. 3B), which was also abrogated by GW9662 (Fig. 3D). Taken together, these data suggested that DHA treatment inhibited LX-2 cell growth by growth arrest in G1 phase with involvement of p27 and p21 via PPARγ.

3.4. Ligand binding to PPARγ via a direct interaction with residues including Ser289, might be required for DHA to inhibit LX-2 cell activation

The above findings suggested that PPARγ might be a direct target of DHA in HSCs. We used a molecular simulation approach to test this hypothesis. The docking data showed that DHA could be embedded into the canonical ligand-binding cavity of PPARγ, which is the exact binding pocket of thiazolidinedione agonists represented by rosiglitazone. Interestingly, in the crystal binding cavity of PPARγ, DHA physically interacted with residues Ser289, His323, Tyr473, and His499, and rosiglitazone interacted with residues Gln286, Ser289, His323, Tyr473, and His499 (Fig. 4A). These results suggested that DHA and rosiglitazone may have very similar binding actions to activate the receptor. Therefore, the canonical thiazolidinedione-binding cavity could be responsible for DHA activation of PPARγ. Subsequently, we used site-directed mutagenesis strategies to confirm whether the interaction with the Ser289 residue was necessary for DHA to exert its effects on HSCs. Western blotting showed that the PPARγ plasmid transfection was successful (Fig. 4B). We observed that DHA suppression of α-SMA and fibronectin expression was significantly abrogated in HSC-LX2 cells transfected with the PPARγ plasmid bearing the Ser289 mutation to alanine (Fig. 4C). Taken together, these data suggested a ligand-binding pattern for DHA activation of PPARγ, leading to the currently observed biological consequences.

3.5. DHA protects the mouse liver from CCl_4-induced injury in a PPARγ-dependent manner

The in vitro results strongly suggested PPARγ dependency of DHA actions on HSC activation. Therefore, we further investigated DHA effects on the CCl_4-treated mouse model with and without PPARγ antagonism. As shown in Fig. 5A, the livers of the normal control (group 1) and DHA control (group 2) had a reddish-brown color and smooth surface, whereas the liver of CCl_4-injected mice (group 3) had a pale color and fine particles on the rough surface. Liver morphology was ameliorated by DHA treatment (group 4), which was abolished by GW9662 addition (group 5). Furthermore, as shown by HE staining in Fig. 5B, DHA treatment resulted in obvious improvement in liver histology of CCl_4-injected mice as evidenced by ameliorated hepatic structural damage, ballooning degeneration, and necrosis. However, GW9662 abolished the improvement of liver histology by DHA. Furthermore, the results of determining serum enzyme levels of ALT and AST verified the role of GW9662 in the interruption of the protective effects of DHA against liver injury (Fig. 5C). Taken together, these results showed that DHA protected the liver from CCl_4-induced injury and suggested its dependence of PPARγ.

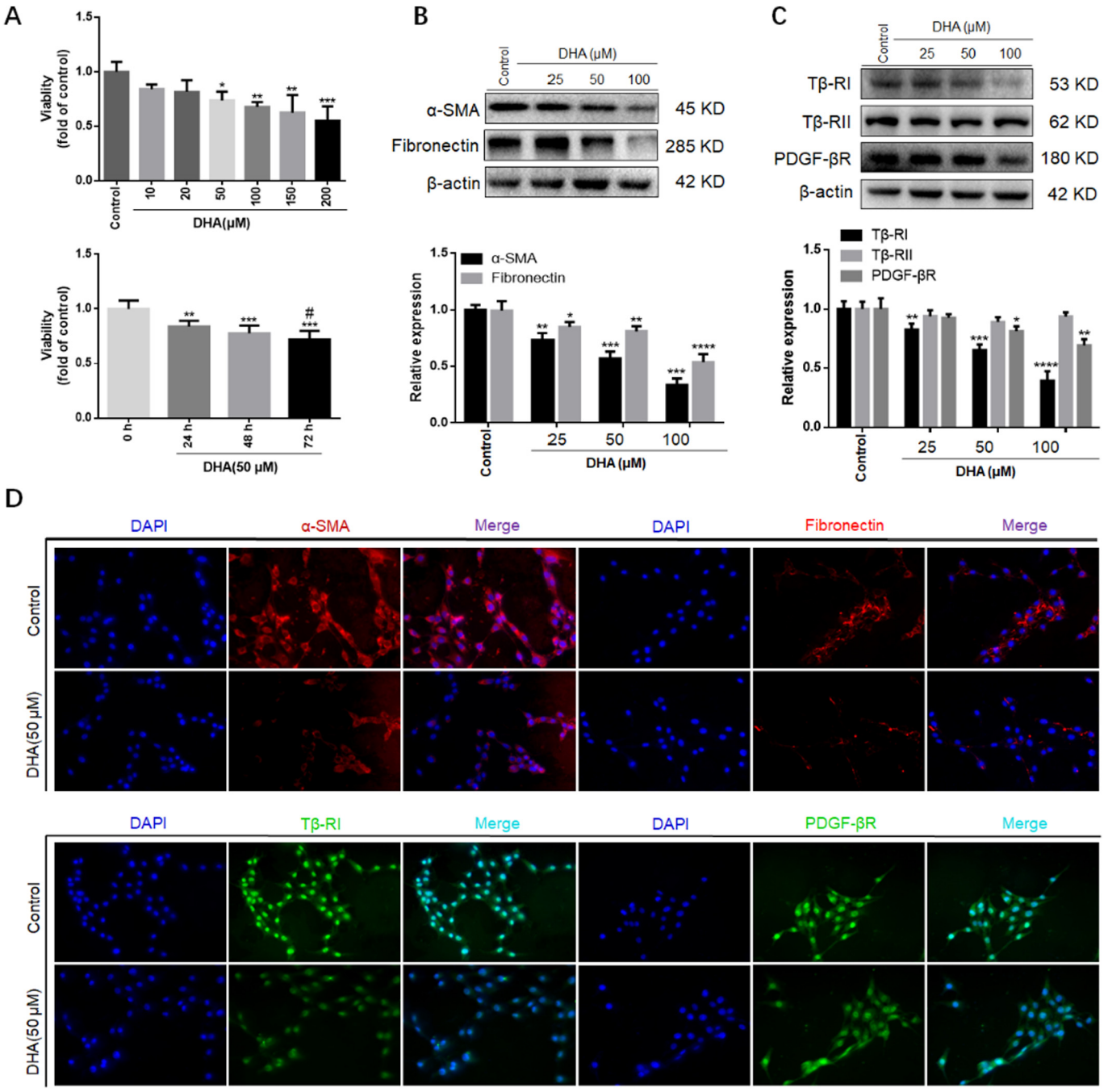

Fig. 1. DHA reduces HSC viability and inhibits HSC activation. (A) MTT assay results. LX-2 cells were treated with the control (0.05% ethanol, v/v) or DHA at the indicated concentrations (10–200 μM) for 24 h (upper panel). *P < 0.05, **P < 0.01, and ***P < 0.001 vs. control. LX-2 cells were also treated with DHA (50 μM) for 24, 48, or 72 h (lower panel). **P < 0.01 vs. 0 h, ***P < 0.001 vs. 0 h, and #P < 0.05 vs. 24 h. (B) Western blot analyses of α-SMA and fibronectin. (C) Western blot analyses of Tβ-RI, Tβ-RII, and PDGF-βR. (D) Immunofluorescence analyses (magnification: × 400) of α-SMA, fibronectin, Tβ-RI, and PDGF-βR. LX-2 cells were treated with the control (0.05% ethanol, v/v) or DHA at 50 μM for 24 h. For western blotting, β-actin was used as an invariant control for equal loading. *P < 0.05, **P < 0.01, ***P < 0.001, and ****P < 0.0001 vs. control.

3.6. DHA ameliorates hepatic fibrogenesis in CCl_4-treated mice in a PPARγ-dependent manner

The main component of the extracellular matrix (ECM) in the fibrotic liver is collagen. We used Masson staining and Sirius Red staining to evaluate the collagen deposition in liver tissue. Both stainings showed severe collagen deposition in the livers of CCl_4-treated mice, typically around the portal area and between lobules. DHA treatment effectively improved the collagen deposition and reduced the formation of fibrous septum (Fig. 6A & B). We also observed that GW9662 diminished the effect of DHA on hepatic fibrogenesis in mice. The content of HYP (almost exclusively in collagens) is an important index to measure collagen production. The results showed that DHA significantly rescued the elevated HYP level in the CCl_4-treated mouse liver, and GW9662 largely abrogated the effect (Fig. 6C). Liver fibrotic indices, including HA, LN, PCIII, and ColIV, in CCl_4-treated mouse serum were also significantly reduced by DHA treatment, which were abolished by GW9662 consistently (Fig. 6D). Immunofluorescence showed that DHA upregulated the level of PPARγ and downregulated the level of α-SMA in HSCs of the mouse liver (Fig. 6E). Collectively,

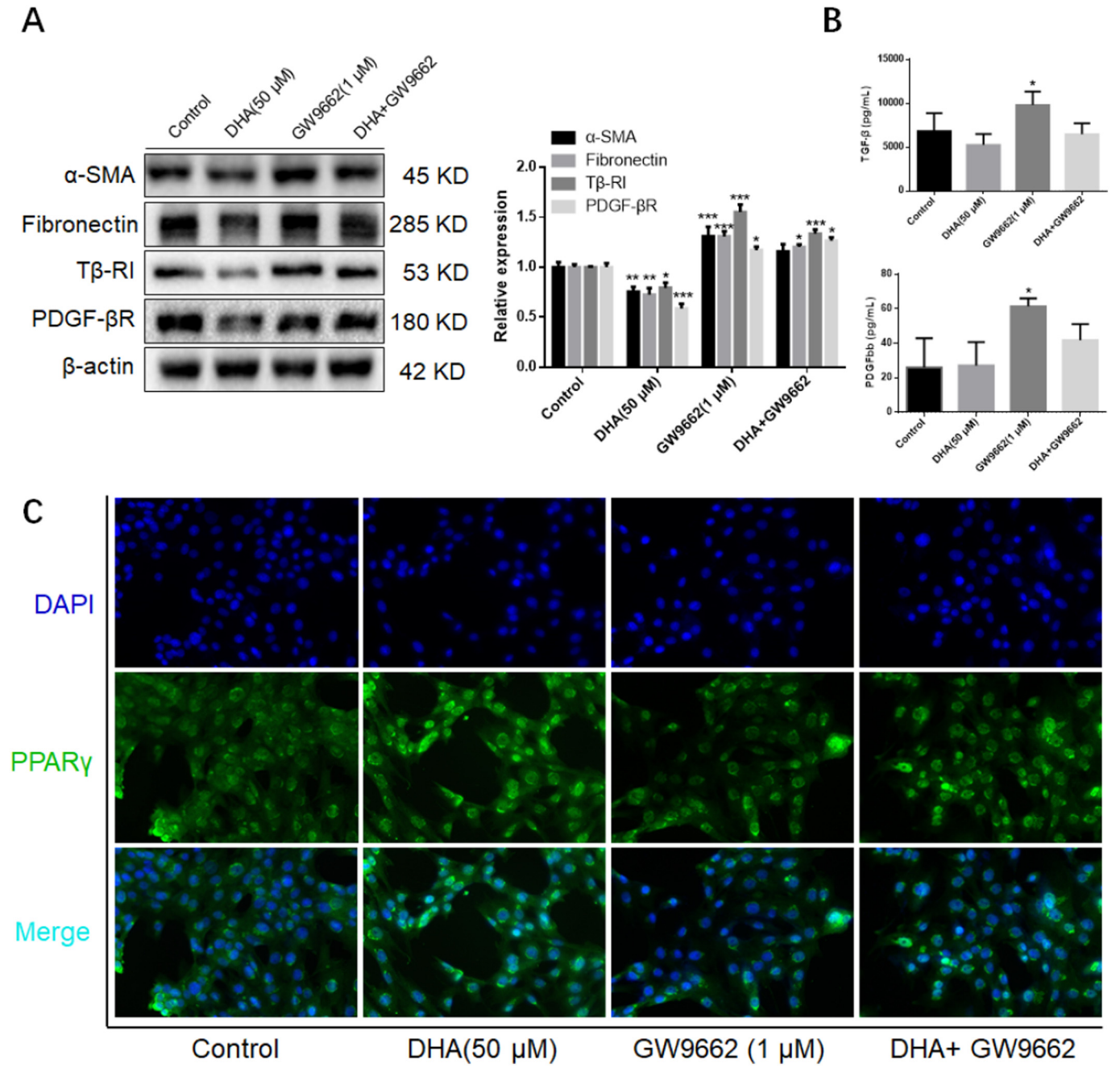

Fig. 2. PPARγ antagonism abolishes DHA effects on inhibiting HSC activation. LX-2 cells were treated with the control (0.05% ethanol), DHA (50 μM), GW9662 (1 μM), or DHA (50 μM) + GW9662 (1 μM). (A) Western blots of α-SMA, fibronectin, Tβ-RI, and PDGF-βR. (B) TGF-β and PDGFbb concentrations in LX-2 cell culture supernatants. (C) Immunofluorescence analysis of PPARγ nuclear translocation in HSC treated with DHA for 24 h (magnification: 400×). For western blotting, β-actin was used as an invariant control for equal loading. *P < 0.05, **P < 0.01, and ***P < 0.001 vs. control.

GW9662 inhibited the DHA effect on improving fibrogenesis in the liver of CCl_4-treated mice, suggesting a role of PPARγ activation in DHA reducing fibrogenesis of the mouse liver.

3.7. DHA suppresses proinflammatory cytokines caused by CCl_4 in a PPARγ-dependent manner

We found that secretion of TGF-β and PDGFbb was elevated by GW9662 in LX-2 cell culture medium (Fig. 2B), suggesting a role of PPARγ in cytokine production. In the in vivo experiments, we found that DHA significantly reduced the elevation of TGF-β and PDGFbb induced by CCl_4, whereas GW9662 abrogated the decreasing effect of DHA on TGF-β and PDGFbb levels in liver tissue (Fig. 7A). TNF-α, IL-6, and IL-8 are critical regulatory factors in liver fibrosis. TNF-α is a cytokine involved in systemic inflammation and stimulates acute inflammation. In the liver, TNF-α is mainly produced by Kupffer cells [19]. Continuous activation of IL-6 can promote collagen production and liver fibrosis [20]. IL-8 is a key proinflammatory cytokine strongly activated in chronic liver diseases [21]. The expression of TNF-α, IL-6, and IL-8 in the liver of CCl_4-treated mice was significantly higher than that in the normal control group. DHA tended to decrease TNF-α production and significantly inhibited the expression of IL-6 and IL-8. GW9662 essentially abolished the inhibitory effect of DHA on the expression of TNF-α, IL-6, and IL-8 (Fig. 7B). CD45 is a common antigen of immune cells, while F4/80 is a marker of macrophages. Therefore, we detected CD45 and F4/80 in liver tissue by immunohistochemistry

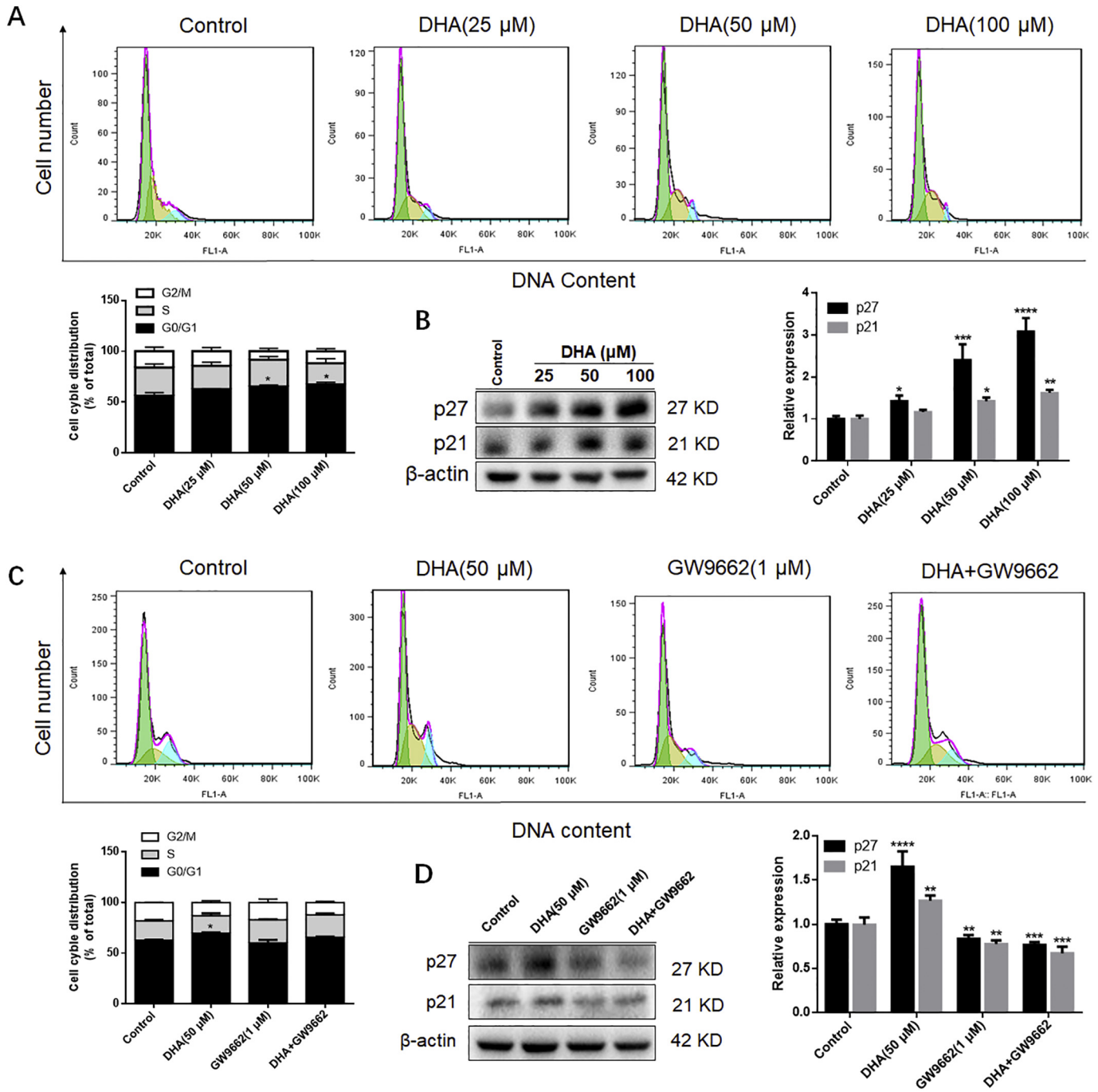

Fig. 3. DHA induces cell cycle arrest in HSCs at G1 phase in a PPARγ-dependent manner. (A) Cell cycle analysis by flow cytometry. LX-2 cells were treated with the control (0.05% ethanol, v/v) or DHA at the indicated concentrations for 24 h. *P < 0.05 vs. control. (B) Western blot analyses of p27 and p21. (C) Cell cycle analysis with GW9662 addition by flow cytometry. *P < 0.05 vs. control. (D) Western blots of p27 and p21 with GW9662 addition. For western blotting, β-actin was used as an invariant control for equal loading. *P < 0.05, **P < 0.01, ***P < 0.001, and ****P < 0.0001 vs. control.

to investigate the effect of DHA on immune cells. We observed that DHA alleviated the infiltration of immune cells and reduced the number of CD45+ and F4/80+ cells in liver tissue, whereas GW9662 considerably diminished these DHA effects (Fig. 7C).

4. Discussion

The safety of DHA has been well studied and confirmed, including the effects of DHA on platelet functions, lipid levels, oxidative potential, glycemic control, and immune functions [22]. In this study, the DHA control group was set to ensure the safety of DHA in the liver. We observed that the livers of DHA-treated mice showed basically no differences from those of normal control mice in terms of morphology and biochemical indicators. Therefore, our study further supported the safety of DHA administration. A study in 2013 showed that fish ω-3 fatty acid supplementation tended to increase liver fibrosis in bile duct ligation rats [23]. However, the fish oil dosage was 0.4% of the rat body weight (i.g.), which was unusually high. It has been suggested that the beneficial effect of DHA is obtained by a daily intake of at least 100 mg for humans [24]. In the current study, we set the dosage (i.g.) for mice at 20 mg/kg, which is equivalent to 1.62 mg/kg in humans [25]. For a man weighting 60 kg, the daily intake would be 97.2 mg, which is

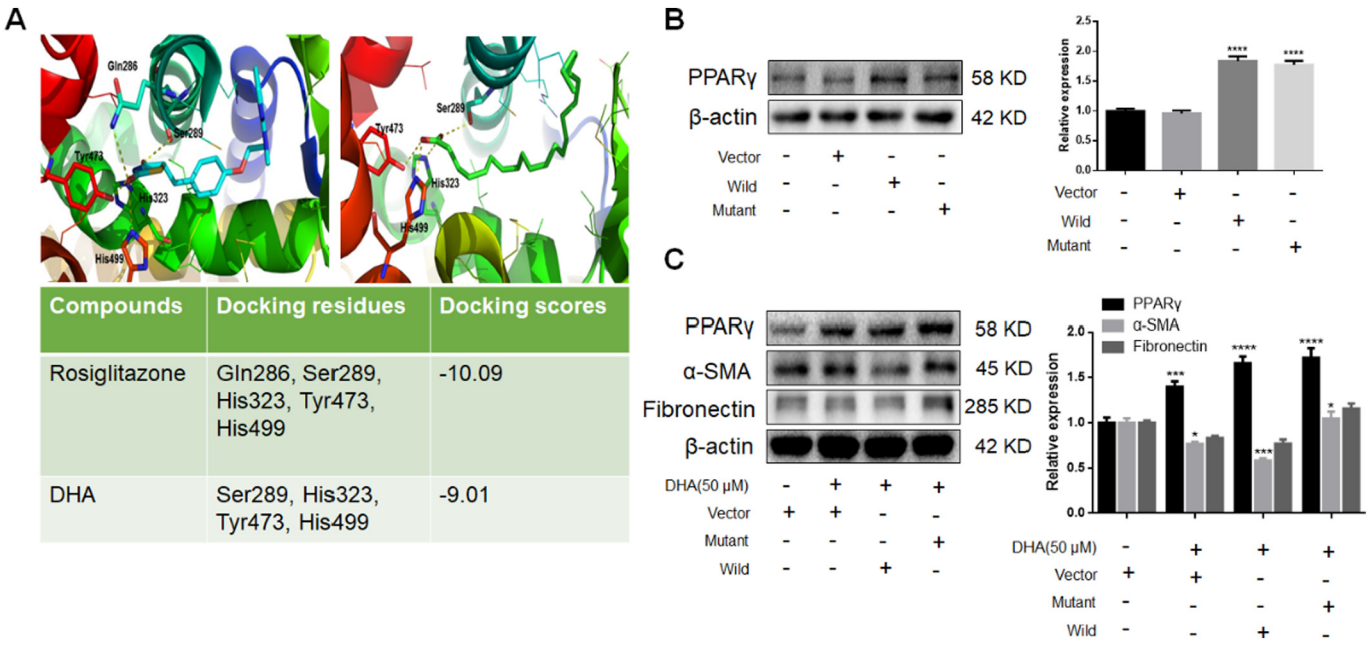

Compounds	Docking residues	Docking scores
Rosiglitazone	Gln286, Ser289, His323, Tyr473, His499	-10.09
DHA	Ser289, His323, Tyr473, His499	-9.01

Fig. 4. Ser289 is required for DHA to bind to PPARγ for activation. (A) Molecular docking images of rosiglitazone (upper left) and DHA (upper right) interactions with the PPARγ-binding pocket. Hydrogen bonds with residues in the binding cavity are represented by yellow-dashed lines. Docking residues and scores are presented in the table (below). (B) LX-2 cells were transfected with the vector plasmid, wildtype PPARγ plasmid, or Ser289 mutant PPARγ plasmid and cultured in DMEM containing 10% FBS for 24 h. Western blotting was performed to determine the PPARγ protein level. (C) LX-2 cells transfected with the vector plasmid, wildtype PPARγ plasmid, or Ser289 mutant PPARγ plasmid were treated with DHA (50 μM) for 24 h. Fibronectin and α-SMA were analyzed by western blotting. For western blotting, β-actin was used as a reference for equivalent loading. *P < 0.05, ***P < 0.001, and ****P < 0.0001 vs. control. (For interpretation of the references to color in this figure legend, the reader is referred to the web version of this article.)

slightly lower than the recommendation. Therefore, our data supported that a relatively low dosage of DHA provides a hepatoprotective effect.

Nuclear receptors are ligand-activated transcription factors that act as sensors for a broad range of natural and synthetic ligands [26]. Targeting nuclear receptors offers exciting new perspectives for the treatment of liver diseases [27]. PPARs are nuclear hormone receptors that act as transcription factors in response to endogenous messengers. They have been found to be important targets in metabolic diseases including obesity, metabolic syndrome, diabetes, and liver diseases [28]. Because DHA might be a potent PPARα agonist [29], we used an irreversible and selective PPARγ inhibitor, GW9662 [30], to investigate the dependence of DHA effects on PPARγ. GW9662 at 10 μM in culture medium has been well established to study the role of PPARγ in several cell lines [31–33]. Therefore, in our in vitro experiments, we used GW9662 at 1 μM to exclude the interference of other PPARs.

In the current study, we observed that DHA activated PPARγ by

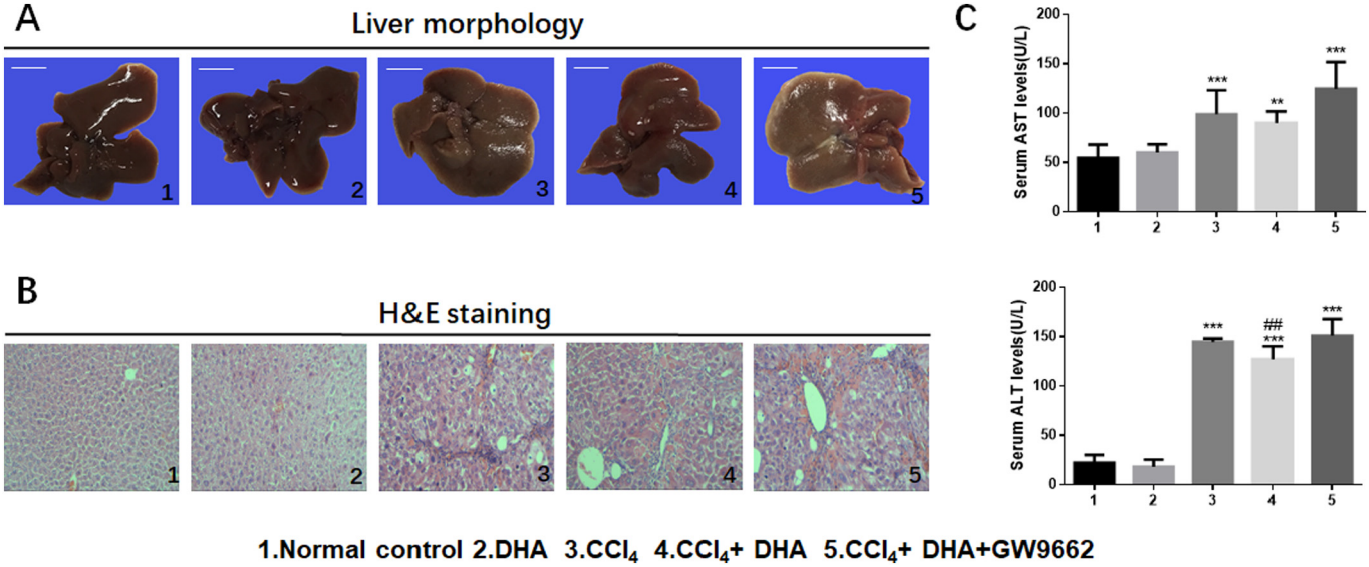

Fig. 5. DHA protects the mouse liver from CCl_4-induced injury in a PPARγ-dependent manner. Mice were grouped as follows: group 1, control (no CCl_4, no treatment); group 2, DHA control (no CCl_4, 20 mg/kg DHA, i.g.); group 3, model (CCl_4, i.p.); group 4, CCl_4 and DHA (20 mg/kg, i.g.); group 5, CCl_4 + DHA (20 mg/kg, i.g.) and GW9662 (3 mg/kg, i.g.). (A) Gross rat liver after sacrifice. Representative photographs are shown. Scale bar: 4 mm. (B) Liver sections were stained with HE for histological examination (magnification: ×200). (C) Determination of serum ALT and AST levels. Data are expressed as the mean ± SEM (n = 8/group); **P < 0.01 vs. group 1, ***P < 0.001 vs. group 1, and ##P < 0.01 vs. group 3.

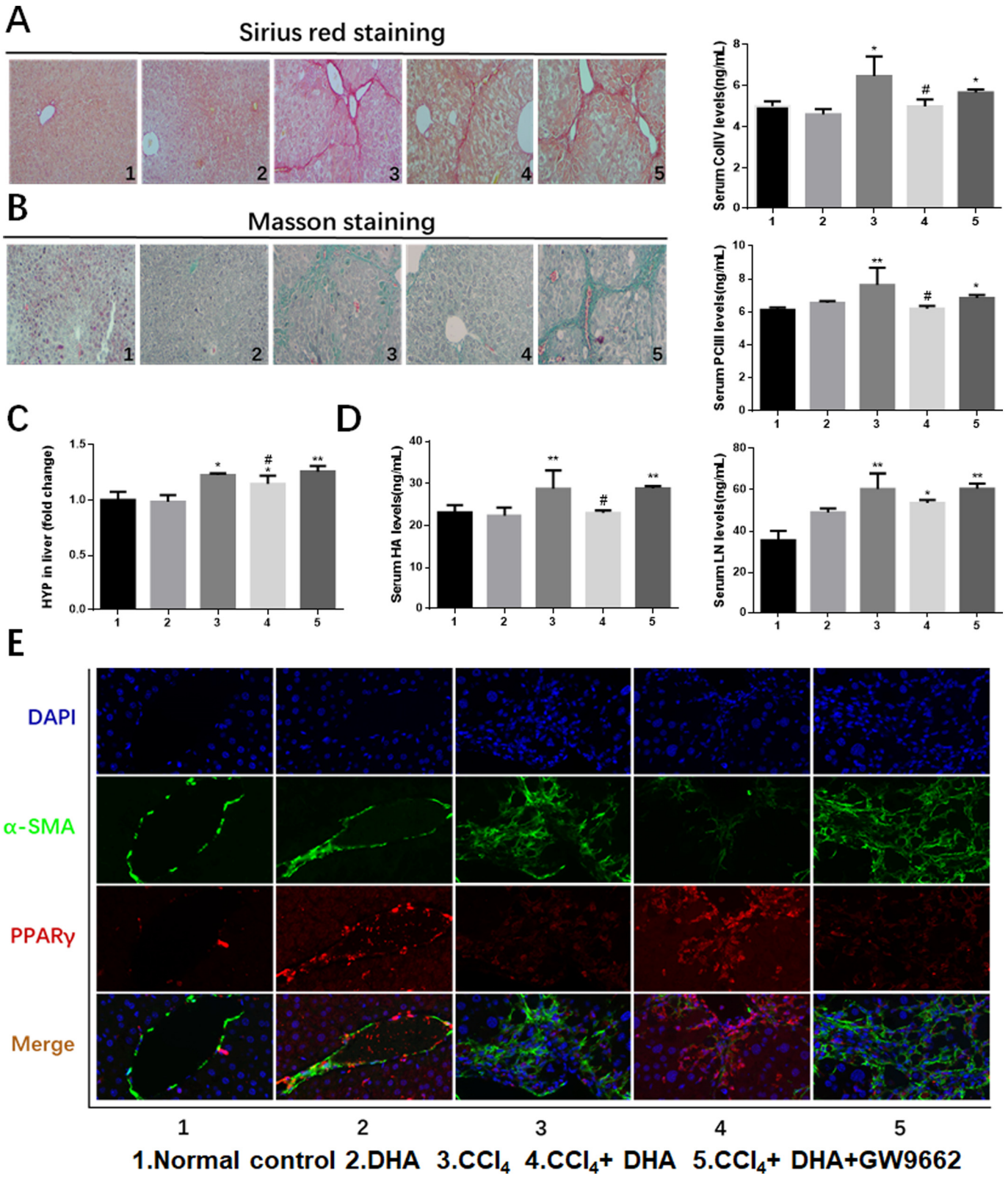

Fig. 6. DHA suppresses CCl_4-induced hepatic fibrogenesis in a PPARγ-dependent manner. Mice were grouped as follows: group 1, control (no CCl_4, no treatment); group 2, DHA control (no CCl_4, 20 mg/kg DHA, i.g.); group 3, model (CCl_4, i.p.); group 4, CCl_4 and DHA (20 mg/kg, i.g.); group 5, CCl_4 + DHA (20 mg/kg, i.g.) and GW9662 (3 mg/kg, i.g.). (A) Liver sections were stained with Sirius red. Representative photographs were shown (magnification: ×200). (B) Liver sections were stained with Masson trichrome. Representative photographs are shown (magnification: ×200). (C) Determination of serum HYP levels in the liver. (D) Determination of serum HA, LN, PCIII, and ColIV levels. (E) Immunofluorescence showing that DHA upregulated PPARγ in HSCs of the mouse liver (magnification: ×200). Data are expressed as the mean ± SEM (n = 8/group); *P < 0.05 vs. group 1, **P < 0.01 vs. group 1, and $^{\#}$P < 0.05 vs. group 3. (For interpretation of the references to color in this figure legend, the reader is referred to the web version of this article.)

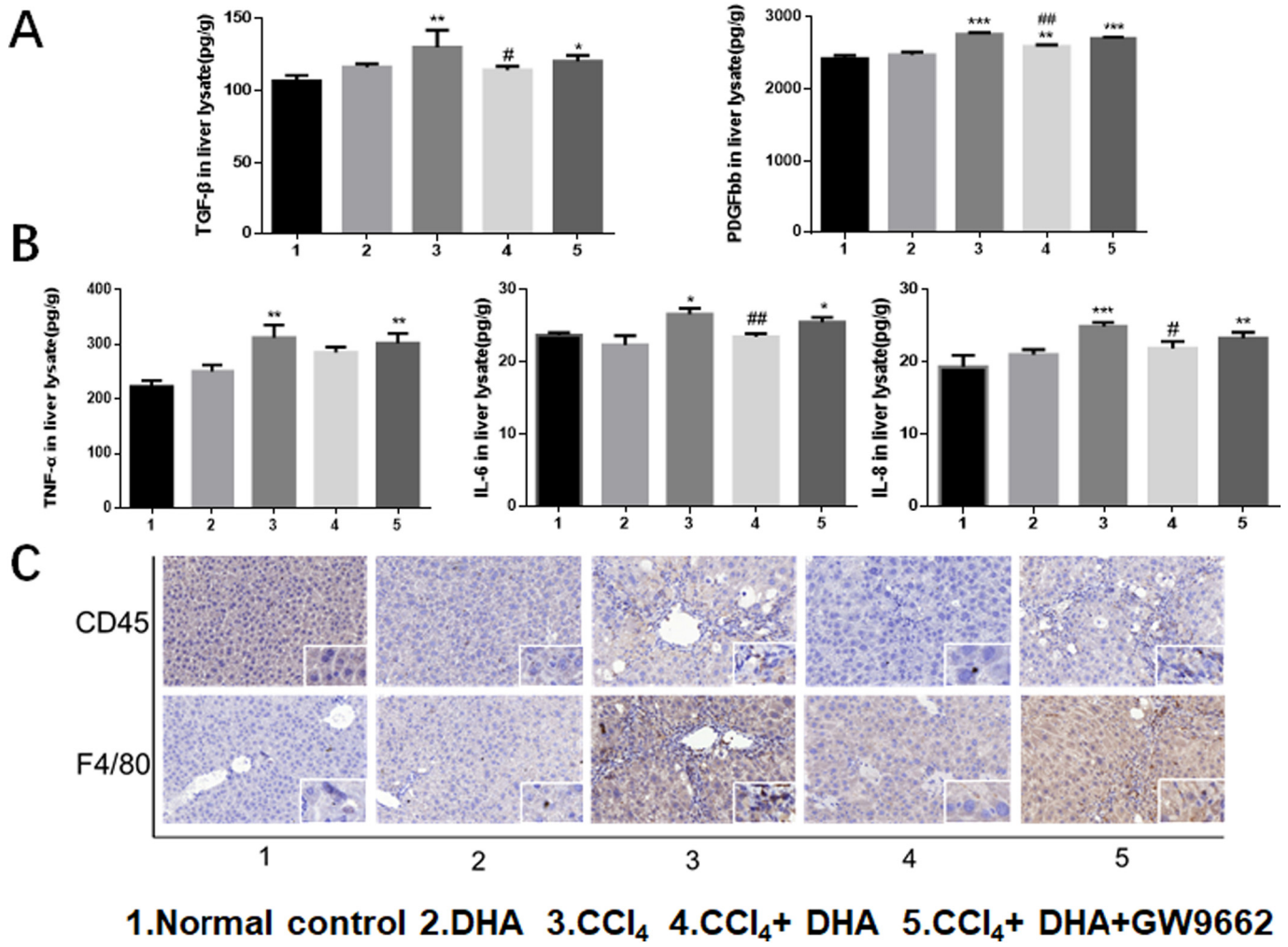

Fig. 7. DHA reduces the levels of proinflammatory cytokines in the CCl_4-treated mouse liver in a PPARγ-dependent manner. Mice were grouped as follows: group 1, control (no CCl_4, no treatment); group 2, DHA control (no CCl_4, 20 mg/kg DHA, i.g.); group 3, model (CCl_4, i.p.); group 4, CCl_4 and DHA (20 mg/kg, i.g.); group 5, CCl_4 + DHA (20 mg/kg, i.g.) and GW9662 (3 mg/kg, i.g.). (A) TGF-β and PDGFbb levels in the liver. (B) TNF-α, IL-6, and IL-8 levels in the liver. (C) Immunohistochemistry of CD45 and F4/80 in the mouse liver (magnification, ×200). Data are expressed as the mean ± SEM (n = 8/group); *P < 0.05 vs. group 1, **P < 0.01 vs. group 1, ***P < 0.001 vs. group 1, #P < 0.05 vs. group 3, and ##P < 0.01 vs. group 3.

stimulating its nuclear translocation in HSCs (Fig. 2C). It is been reported that PPARγ activation inhibits TGF-β induced corneal myofibroblast transformation [34] and PDGF-induced vascular smooth muscle cell proliferation [35]. In this study, we found that DHA downregulated Tβ-RI and PDGF-βR in HSC-LX2 cells. However, we did not observe an obvious alteration of the production of TGF-β or PDGFbb induced by DHA. Interestingly, the PPARγ selective inhibitor GW9662 significantly elevated TGF-β and PDGFbb levels in the HSC culture medium (Fig. 2B). Our data implied that DHA might interfere with PPARγ/TGF-β and PPARγ/PDGF signaling by downregulating their receptors, Tβ-RI and PDGF-βR, in HSCs. Furthermore, our data indicated that PPARγ antagonism not only abolishes DHA effects on the cytokine-transmitting receptors, but also strongly enhances the profibrogenic signals by increasing cytokine expression, suggesting a role of endogenous PPARγ in modulating profibrogenic cytokines.

DHA has been reported to have a hepatoprotective effect through multiple mechanisms [36–39]. HSC activation is now well established as a central driver of liver fibrosis [40]. However, DHA effects on HSCs were largely unknown.

In this study, we first aimed to confirm whether DHA has a direct effect on HSCs. As shown by our data, 50 μM DHA significantly reduced LX-2 cell viability in vitro. DHA also downregulated the expression of marker proteins of HSC activation. Furthermore, we found that DHA treatment increased p27 and p21 levels, and arrested the LX-2 cell cycle at G1 phase. These evidences demonstrated that inhibiting HSC activation is one of the mechanisms underlying DHA-mediated attenuation of liver fibrosis. More importantly, with pharmaceutic antagonism of PPARγ, DHA effects on HSCs were largely abolished, suggesting that PPARγ activation in HSCs is vital for DHA to exert its effect. Based on the above observations, we further speculated a direct interaction between DHA and PPARγ. This speculation was supported by molecular docking evidence showing that DHA could bind to the canonical ligand-binding pocket of PPARγ via hydrogen bonding with Ser289, His323, Tyr473, and His499, which were largely overlapped with the bonding residues of rosiglitazone. Interestingly, it is reported that rosiglitazone inhibits HSC activation in vitro and in vivo [41,42], characterized by decreased HSC proliferation and α-SMA expression, similar to DHA. Therefore, we wanted to further confirm the role of the bonding residues in DHA activating PPARγ. The virtual docking data were then verified by mutagenesis assays, the data of which suggested that bonding with Ser289 was required for DHA to activate PPARγ to inhibit HSC activation. Considering that rosiglitazone also interacted with Ser289, we speculated that the interaction with Ser289 was conserved for ligand activation of PPARγ. It is noteworthy that GW9662 inhibits PPARγ by covalently reacted with the Cys285 residue in the PPARγ ligand-binding domain [30], which is closely adjacent to the Ser289

residue. Accordingly, we inferred that the covalent modification of Cys285 might interrupt the hydrogen bonding of DHA and Ser289, resulting the loss of DHA-mediated suppression of PPARγ activation. These data confirmed the important role of Ser289 in DHA activating PPARγ. The role of the other residues needs to be verified in our future studies. We subsequently used a classical CCl_4-induced liver fibrosis model in mice to establish the in vivo correlation. As a result, liver fibrosis in CCl_4-treated mice was attenuated by chronic DHA administration evidenced by the ameliorated liver histological state, decreased collagen deposition, and suppressed inflammation. Furthermore, the DHA actions on liver fibrosis were abrogated by GW9662 in vivo, which is consistent with the in vitro data. Taken together, these results indicated the dependency of PPARγ for DHA actions on liver fibrosis.

PPARγ activation was also reported to upregulate p27 and p21 and cause G0/G1 arrest in several human hepatoma cancer cell lines [43]. It was found that p27 upregulation induced by PPARγ agonist might occur by reduced proteosomal degradation and accumulation of p27 via downregulation of Skp2 [43,44], which is required for the ubiquitin-dependent degradation of p27 [45]. Serval studies found that PPARγ activation increases p21 mRNA level [46–48]. In human lung carcinoma cells, the induction of p21 gene expression by PPARγ ligands was found mediated through increased transcriptional activation [48]. Further, it was reported that PPARγ activation enhances nuclear localization of p21 [43].

It was observed that PPARγ activation inhibits cytokine synthesis pre-translationally. The accumulation of TNF-α mRNA in human peripheral blood monocytes was found inhibited by PPARγ agonists. Also, the TNF-α promoter activity was significantly inhibited by 15d-PGJ2 and troglitazone in U937 cells [49]. A trans-repression mechanism explaining an intranuclear crosstalk between PPAR and transcription factors on the promoters of inflammatory genes was proposed and verified by preponderance of evidence [50]. Synthetic and natural PPARγ agonists block transactivation of transcription factors NF-κB and 5′-CCAAT/enhancer–binding protein β (C/EBPβ) to interfere with IL-6 transcription and production [51]. Thus, we assumed that DHA activated PPARγ to inhibit cytokine productions in HSC probably via a trans-repression mechanism.

The relationship between PUFA and non-alcoholic steatohepatitis (NASH) was also studied by several groups. It was found that well-defined subjects with either healthy liver, simple steatosis, or NASH showed distinct hepatic gene expression profiles (GEO accession number: GSE89632) including genes involved in unsaturated fatty acid metabolism, which suggested that gene expression influences PUFA content differently depending on disease severity [52]. Another group reported a significant enrichment of genes involved in the multi-step catalysis of long-chain PUFA, including Δ-5 and Δ-6 desaturases in human NASH patients (GEO accession number: GSE37031), resulting in an increased ω-6 to ω-3 ratio [53]. Further, they also found that both the endogenous conversion of ω-6 into ω-3 fatty acids (in a *fat-1* transgenic mice model) and an exogenous ω-3-enriched diet produced significant reduction in steatosis, necroinflammation and lipid peroxidation, accompanied by attenuated expression of genes involved in inflammation, fatty acid uptake and lipogenesis in mice. Therefore, ω-3 fatty acids supplement might be a strategy for NASH treatment.

We also tried to address the relationship between DHA-dependent and PPARγ-dependent gene expression by Coremine Medical online (http://www.coremine.com/medical/), which is designed to seek information on health, medicine, and biology. 276 genes were found significantly correlated to both DHA and non-alcoholic fatty liver disease (NAFLD) (Table S1); 335 genes were found significantly correlated to both rosiglitazone (represents PPARγ activation) and NAFLD (Table S2). Surprisingly, 169 genes were overlapped (Table S3) among them. Those overlapped genes were mainly related to lipid metabolic process (Fig. S1) according to a functional annotation analysis with DAVID Bioinformatics Resources 6.7 [54]. Thus, these findings also implied a role of PPARγ in regulating lipid metabolism in NAFLD.

In summary, we found that DHA activates PPARγ in a classical thiazolidinedione agonist-binding mode to inhibit HSC activation, leading to the attenuation of liver fibrosis. Our findings reveal new mechanisms of the hepatoprotective actions of DHA and provide novel evidence of PPARγ activation with therapeutic implications for liver fibrosis.

Declaration of competing interest

The authors declare no conflict of interest.

Acknowledgments

This work was supported by the Scientific Research Foundation of Third Institute of Oceanography, Ministry of Natural Resources [grant number 2018020], the Science and Technology Plan Program of Fujian Province [grant number 2017Y0061], Xiamen Marine Economic Innovation and Development Demonstration Project [grant number 16CZP012SF04], and the National Natural Science Foundation of China [grant numbers 31401210, 31571455, and 81600483].

Appendix A. Supplementary data

Supplementary data to this article can be found online at https://doi.org/10.1016/j.intimp.2019.105816.

References

[1] L. Campana, J.P. Iredale, Regression of liver fibrosis, Semin. Liver Dis. 37 (1) (2017) 1–10.
[2] D. Povero, C. Busletta, E. Novo, L.V. di Bonzo, S. Cannito, C. Paternostro, M. Parola, Liver fibrosis: a dynamic and potentially reversible process, Histol. Histopathol. 25 (8) (2010) 1075–1091.
[3] T. Higashi, S.L. Friedman, Y. Hoshida, Hepatic stellate cells as key target in liver fibrosis, Adv. Drug Deliv. Rev. 121 (2017) 27–42.
[4] S. Hazra, T. Miyahara, R.A. Rippe, H. Tsukamoto, PPAR gamma and hepatic stellate cells, Comp. Hepatol. 3 (Suppl. 1) (2004) S7.
[5] Z. Wang, J.P. Xu, Y.C. Zheng, W. Chen, Y.W. Sun, Z.Y. Wu, M. Luo, Peroxisome proliferator-activated receptor gamma inhibits hepatic fibrosis in rats, Hepatobiliary Pancreat. Dis. Int. 10 (1) (2011) 64–71.
[6] R. Kones, S. Howell, U. Rumana, n − 3 polyunsaturated fatty acids and cardiovascular disease: principles, practices, pitfalls, and promises - a contemporary review, Med. Princ. Pract. 26 (6) (2017) 497–508.
[7] M. Firlag, M. Kamaszewski, K. Gaca, D. Adamek, B. Balasinska, The neuroprotective effect of long-term n − 3 polyunsaturated fatty acids supplementation in the cerebral cortex and hippocampus of aging rats, Folia Neuropathol. 51 (3) (2013) 235–242.
[8] J. He, K. Bai, B. Hong, F. Zhang, S. Zheng, Docosahexaenoic acid attenuates carbon tetrachloride-induced hepatic fibrosis in rats, Int. Immunopharmacol. 53 (2017) 56–62.
[9] R.K. Moreira, Hepatic stellate cells and liver fibrosis, Arch. Pathol. Lab. Med. 131 (11) (2007) 1728–1734.
[10] O.A. Gani, Are fish oil omega-3 long-chain fatty acids and their derivatives peroxisome proliferator-activated receptor agonists? Cardiovasc. Diabetol. 7 (2008) 6.
[11] Q. Chen, L. Chen, X. Wu, F. Zhang, H. Jin, C. Lu, J. Shao, D. Kong, L. Wu, S. Zheng, Dihydroartemisinin prevents liver fibrosis in bile duct ligated rats by inducing hepatic stellate cell apoptosis through modulating the PI3K/Akt pathway, IUBMB Life 68 (3) (2016) 220–231.
[12] L. Xu, A.Y. Hui, E. Albanis, M.J. Arthur, S.M. O'Byrne, W.S. Blaner, P. Mukherjee, S.L. Friedman, F.J. Eng, Human hepatic stellate cell lines, LX-1 and LX-2: new tools for analysis of hepatic fibrosis, Gut 54 (1) (2005) 142–151.
[13] G. Carpino, S. Morini, S. Ginanni Corradini, A. Franchitto, M. Merli, M. Siciliano, F. Gentili, A. Onetti Muda, P. Berloco, M. Rossi, A.F. Attili, E. Gaudio, Alpha-SMA expression in hepatic stellate cells and quantitative analysis of hepatic fibrosis in cirrhosis and in recurrent chronic hepatitis after liver transplantation, digestive and liver disease: official journal of the Italian Society of Gastroenterology and the Italian Association for the, Stud. Liver 37 (5) (2005) 349–356.
[14] X.Y. Liu, R.X. Liu, F. Hou, L.J. Cui, C.Y. Li, C. Chi, E. Yi, Y. Wen, C.H. Yin, Fibronectin expression is critical for liver fibrogenesis in vivo and in vitro, Mol. Med. Rep. 14 (4) (2016) 3669–3675.
[15] A. Biernacka, M. Dobaczewski, N.G. Frangogiannis, TGF-beta signaling in fibrosis, Growth Factors 29 (5) (2011) 196–202.
[16] P. Czochra, B. Klopcic, E. Meyer, J. Herkel, J.F. Garcia-Lazaro, F. Thieringer, P. Schirmacher, S. Biesterfeld, P.R. Galle, A.W. Lohse, S. Kanzler, Liver fibrosis induced by hepatic overexpression of PDGF-B in transgenic mice, J. Hepatol. 45 (3) (2006) 419–428.
[17] J.C. Bonner, Regulation of PDGF and its receptors in fibrotic diseases, Cytokine

Growth Factor Rev. 15 (4) (2004) 255–273.
[18] B.H. Davis, Transforming growth factor beta responsiveness is modulated by the extracellular collagen matrix during hepatic ito cell culture, J. Cell. Physiol. 136 (3) (1988) 547–553.
[19] H. Kawaratani, T. Tsujimoto, A. Douhara, H. Takaya, K. Moriya, T. Namisaki, R. Noguchi, H. Yoshiji, M. Fujimoto, H. Fukui, The effect of inflammatory cytokines in alcoholic liver disease, Mediat. Inflamm. 2013 (2013) 495156.
[20] I. Choi, H.S. Kang, Y. Yang, K.H. Pyun, IL-6 induces hepatic inflammation and collagen synthesis in vivo, Clin. Exp. Immunol. 95 (3) (1994) 530–535.
[21] H.W. Zimmermann, S. Seidler, N. Gassler, J. Nattermann, T. Luedde, C. Trautwein, F. Tacke, Interleukin-8 is activated in patients with chronic liver diseases and associated with hepatic macrophage accumulation in human liver fibrosis, PLoS One 6 (6) (2011) e21381.
[22] E.L. Lien, Toxicology and safety of DHA, Prostaglandins Leukot. Essent. Fat. Acids 81 (2–3) (2009) 125–132.
[23] C.C. Chen, C.Y. Ho, H.C. Chaung, Y.L. Tain, C.S. Hsieh, F.Y. Kuo, C.Y. Yang, L.T. Huang, Fish omega-3 fatty acids induce liver fibrosis in the treatment of bile duct-ligated rats, Dig. Dis. Sci. 58 (2) (2013) 440–447.
[24] H. Rice, A. Ismail, Fish oils in human nutrition: history and current status, Fish and Fish Oil in Health and Disease Prevention, Elsevier, 2016, pp. 75–84.
[25] A.B. Nair, S. Jacob, A simple practice guide for dose conversion between animals and human, J. Basic Clin. Pharm. 7 (2) (2016) 27–31.
[26] M. Trauner, E. Halilbasic, Nuclear receptors as new perspective for the management of liver diseases, Gastroenterology 140 (4) (2011) 1120–1125 e1-12.
[27] F. Zhang, S. Lu, J. He, H. Jin, F. Wang, L. Wu, J. Shao, A. Chen, S. Zheng, Ligand activation of PPARgamma by ligustrazine suppresses pericyte functions of hepatic stellate cells via SMRT-mediated transrepression of HIF-1alpha, Theranostics 8 (3) (2018) 610–626.
[28] L.B. Ferguson, L. Zhang, S. Wang, C. Bridges, R.A. Harris, I. Ponomarev, Peroxisome proliferator activated receptor agonists modulate transposable element expression in brain and liver, Front. Mol. Neurosci. 11 (2018) 331.
[29] Q.N. Diep, R.M. Touyz, E.L. Schiffrin, Docosahexaenoic acid, a peroxisome proliferator-activated receptor-alpha ligand, induces apoptosis in vascular smooth muscle cells by stimulation of p38 mitogen-activated protein kinase, Hypertension 36 (5) (2000) 851–855.
[30] L.M. Leesnitzer, D.J. Parks, R.K. Bledsoe, J.E. Cobb, J.L. Collins, T.G. Consler, R.G. Davis, E.A. Hull-Ryde, J.M. Lenhard, L. Patel, K.D. Plunket, J.L. Shenk, J.B. Stimmel, C. Therapontos, T.M. Willson, S.G. Blanchard, Functional consequences of cysteine modification in the ligand binding sites of peroxisome proliferator activated receptors by GW9662, Biochemistry 41 (21) (2002) 6640–6650.
[31] T.S. Pavlov, V. Levchenko, A.V. Karpushev, A. Vandewalle, A. Staruschenko, Peroxisome proliferator-activated receptor gamma antagonists decrease Na+ transport via the epithelial Na+ channel, Mol. Pharmacol. 76 (6) (2009) 1333–1340.
[32] J. Yan, H. Yang, G. Wang, L. Sun, Y. Zhou, Y. Guo, Z. Xi, X. Jiang, Autophagy augmented by troglitazone is independent of EGFR transactivation and correlated with AMP-activated protein kinase signaling, Autophagy 6 (1) (2010) 67–73.
[33] S.Z. Dong, S.P. Zhao, Z.H. Wu, J. Yang, X.Z. Xie, B.L. Yu, S. Nie, Curcumin promotes cholesterol efflux from adipocytes related to PPARgamma-LXRalpha-ABCA1 passway, Mol. Cell. Biochem. 358 (1–2) (2011) 281–285.
[34] K.I. Jeon, A. Kulkarni, C.F. Woeller, R.P. Phipps, P.J. Sime, H.B. Hindman, K.R. Huxlin, Inhibitory effects of PPARgamma ligands on TGF-beta1-induced corneal myofibroblast transformation, Am. J. Pathol. 184 (5) (2014) 1429–1445.
[35] I. Osman, L. Segar, Pioglitazone, a PPARgamma agonist, attenuates PDGF-induced vascular smooth muscle cell proliferation through AMPK-dependent and AMPK-independent inhibition of mTOR/p70S6K and ERK signaling, Biochem. Pharmacol. 101 (2016) 54–70.
[36] W.Y. Chen, S.Y. Lin, H.C. Pan, S.L. Liao, Y.H. Chuang, Y.J. Yen, S.Y. Lin, C.J. Chen, Beneficial effect of docosahexaenoic acid on cholestatic liver injury in rats, J. Nutr. Biochem. 23 (3) (2012) 252–264.
[37] K.A. Lytle, C.M. Depner, C.P. Wong, D.B. Jump, Docosahexaenoic acid attenuates Western diet-induced hepatic fibrosis in Ldlr−/− mice by targeting the TGFbeta-Smad3 pathway, J. Lipid Res. 56 (10) (2015) 1936–1946.
[38] A. Gonzalez-Periz, A. Planaguma, K. Gronert, R. Miquel, M. Lopez-Parra, E. Titos, R. Horrillo, N. Ferre, R. Deulofeu, V. Arroyo, J. Rodes, J. Claria, Docosahexaenoic acid (DHA) blunts liver injury by conversion to protective lipid mediators: protectin D1 and 17S-hydroxy-DHA, FASEB J. 20 (14) (2006) 2537–2539.
[39] K. Zhang, Y. Chang, Z. Shi, X. Han, Y. Han, Q. Yao, Z. Hu, H. Cui, L. Zheng, T. Han, W. Hong, Omega-3 PUFAs ameliorate liver fibrosis and inhibit hepatic stellate cells proliferation and activation by promoting YAP/TAZ degradation, Sci. Rep. 6 (2016) 30029.
[40] T. Tsuchida, S.L. Friedman, Mechanisms of hepatic stellate cell activation, Nat. Rev. Gastroenterol. Hepatol. 14 (7) (2017) 397–411.
[41] Y.T. Guo, X.S. Leng, T. Li, J.R. Peng, S.H. Song, L.F. Xiong, Z.Z. Qin, Effect of ligand of peroxisome proliferator-activated receptor gamma on the biological characters of hepatic stellate cells, World J. Gastroenterol. 11 (30) (2005) 4735–4739.
[42] S.C. Zhi, S.Z. Chen, Y.Y. Li, J.J. Li, Y.H. Zheng, F.X. Yu, Rosiglitazone inhibits activation of hepatic stellate cells via up-regulating micro-RNA-124-3p to alleviate hepatic fibrosis, Dig. Dis. Sci. 64 (6) (2019) 1560–1570.
[43] H. Koga, S. Sakisaka, M. Harada, T. Takagi, S. Hanada, E. Taniguchi, T. Kawaguchi, K. Sasatomi, R. Kimura, O. Hashimoto, T. Ueno, H. Yano, M. Kojiro, M. Sata, Involvement of p21(WAF1/Cip1), p27 (Kip1), and p18(INK4c) in troglitazone-induced cell-cycle arrest in human hepatoma cell lines, Hepatology 33 (5) (2001) 1087–1097.
[44] V. Agosti, D. Talarico, A. Urzino, R.V. Murthi, A.A.R. Nocera, E.D. Giovannone, PPAR-γ agonists induce growth arrest of kit/AML1-ETO leukemia cells acting on diverse pathways, Blood 124 (21) (2014) 5211.
[45] A.C. Carrano, E. Eytan, A. Hershko, M. Pagano, SKP2 is required for ubiquitin-mediated degradation of the CDK inhibitor p27, Nat. Cell Biol. 1 (4) (1999) 193–199.
[46] R.F. Morrison, S.R. Farmer, Role of PPARgamma in regulating a cascade expression of cyclin-dependent kinase inhibitors, p18(INK4c) and p21 (Waf1/Cip1), during adipogenesis, J. Biol. Chem. 274 (24) (1999) 17088–17097.
[47] W.A. Miller, B.R. Wuertz, F.G. Ondrey, PPARgamma-mediated p21 induction in aerodigestive preneoplastic cell lines, Ann. Otol. Rhinol. Laryngol. 127 (10) (2018) 677–686.
[48] S. Han, N. Sidell, P.B. Fisher, J. Roman, Up-regulation of p21 gene expression by peroxisome proliferator-activated receptor gamma in human lung carcinoma cells, Clin. Cancer Res. 10 (6) (2004) 1911–1919.
[49] C. Jiang, A.T. Ting, B. Seed, PPAR-gamma agonists inhibit production of monocyte inflammatory cytokines, Nature 391 (6662) (1998) 82–86.
[50] G. Pascual, A.L. Fong, S. Ogawa, A. Gamliel, A.C. Li, V. Perissi, D.W. Rose, T.M. Willson, M.G. Rosenfeld, C.K. Glass, A SUMOylation-dependent pathway mediates transrepression of inflammatory response genes by PPAR-gamma, Nature 437 (7059) (2005) 759–763.
[51] L.H. Wang, X.Y. Yang, X. Zhang, W.L. Farrar, Inhibition of adhesive interaction between multiple myeloma and bone marrow stromal cells by PPARgamma cross talk with NF-kappaB and C/EBP, Blood 110 (13) (2007) 4373–4384.
[52] B.M. Arendt, E.M. Comelli, D.W. Ma, W. Lou, A. Teterina, T. Kim, S.K. Fung, D.K. Wong, I. McGilvray, S.E. Fischer, J.P. Allard, Altered hepatic gene expression in nonalcoholic fatty liver disease is associated with lower hepatic n−3 and n−6 polyunsaturated fatty acids, Hepatology 61 (5) (2015) 1565–1578.
[53] C. Lopez-Vicario, A. Gonzalez-Periz, B. Rius, E. Moran-Salvador, V. Garcia-Alonso, J.J. Lozano, R. Bataller, M. Cofan, J.X. Kang, V. Arroyo, J. Claria, E. Titos, Molecular interplay between Delta5/Delta6 desaturases and long-chain fatty acids in the pathogenesis of non-alcoholic steatohepatitis, Gut 63 (2) (2014) 344–355.
[54] W. Huang da, B.T. Sherman, R.A. Lempicki, Systematic and integrative analysis of large gene lists using DAVID bioinformatics resources, Nat. Protoc. 4 (1) (2009) 44–57.